Cureus
Part of SPRINGER NATURE

Open Access Case Report

Adult Langerhans Cell Histiocytosis Mimicking Miliary Tuberculosis: A Multimodality Imaging Case Report

Review began 10/13/2026
Review ended 11/08/2026
Published 11/16/2026

© **Copyright** 2026
Burundi et al. This is an open access article distributed under the terms of the Creative Commons Attribution License CC-BY 4.0., which permits unrestricted use, distribution, and reproduction in any medium, provided the original author and source are credited.

DOI: 10.7759/cureus.119723

Dulcis I. Burundi [1], Pascale Bohy [1]

1. Radiology, Erasmus Hospital, Brussels, BEL

Corresponding author: Dulcis I. Burundi, diburundi@gmail.com

Abstract

Langerhans cell histiocytosis (LCH), historically known as histiocytosis X, is a rare disorder that can present as single-system or multisystem disease. In adults, it predominantly occurs in current or former smokers, who typically have upper- and mid-lung micronodules, nodules, or cavitated nodules and cysts. In multisystem disease, bone involvement is a recognized extrapulmonary manifestation that can lead to an initial misdiagnosis of infection or metastatic disease.

This case describes a 62-year-old woman presenting with chronic lower back pain. Imaging initially revealed a lytic vertebral lesion and pulmonary micronodules and nodules with a miliary distribution, identified during an oncological workup using whole-body fluorodeoxyglucose positron emission tomography/computed tomography (FDG PET/CT) and thoracoabdominal CT. Extensive microbiological investigations led to invasive diagnostic procedures, including bronchoalveolar lavage, transbronchial biopsy, and vertebral biopsy, which were initially negative. Miliary tuberculosis (TB) was initially suspected, and empirical four-drug antituberculous treatment was initiated in May 2022. After approximately six weeks, no significant radiographic improvement was observed. Follow-up FDG PET/CT in July 2022 demonstrated a mixed metabolic response, including a new FDG-avid vertebral lesion. Antituberculous treatment was discontinued after approximately 11 weeks because of the absence of a favorable overall imaging response and negative mycobacterial cultures.

Subsequent evolution of the pulmonary nodules, with cavitation and cyst formation, prompted reconsideration of the diagnosis. Reassessment of the pulmonary biopsy showed numerous CD1a- and S100-positive cells, and molecular testing later identified a BRAF p.V600E/D alteration, further supporting the diagnosis of LCH. Following smoking cessation, subsequent imaging demonstrated marked improvement in the pulmonary abnormalities and metabolic normalization of the previously active osseous lesions.

This case illustrates the value of serial CT imaging and FDG PET/CT in redirecting the diagnostic approach when adult LCH initially mimics miliary TB.

Categories: Nuclear Medicine, Radiology, Pulmonology
Keywords: braf mutation, fdg pet/ct, langerhans cell histiocytosis(lch), miliary tuberculosis (tb), multiple pulmonary nodules, pulmonary langerhans cell histiocytosis

Introduction

Langerhans cell histiocytosis (LCH), historically known as histiocytosis X, is a rare clonal histiocytic disorder defined by its characteristic cell phenotype and molecular alterations and may involve one or several organ systems [1]. The incidence in adults is estimated at approximately one per million per year, whereas in children, it is estimated at 4.46 per million per year [2]. Clinical manifestations of LCH vary according to the organs involved. Adult pulmonary LCH occurs predominantly in current or former smokers and may present with cough, exertional dyspnea, chest pain, or spontaneous pneumothorax, although some patients remain asymptomatic [3,4]. On high-resolution computed tomography (HRCT), the classical pattern consists of an evolving combination of micronodules, nodules, cavitated nodules, and irregular cysts, with an upper- and mid-lung predominance [3,4]. Early disease, however, may be predominantly nodular and can mimic tuberculosis (TB), sarcoidosis, or hematogenous metastases [5]. Unlike the typically diffuse, randomly distributed micronodules of miliary TB, pulmonary LCH usually demonstrates upper- and mid-lung predominance, often with relative sparing of the lung bases. Extrapulmonary manifestations, particularly bone involvement characterized by osteolytic lesions, are also well recognized and may further complicate the differential diagnosis [6]. LCH is characterized by the accumulation of abnormal myeloid-derived dendritic cells, frequently associated with activation of the mitogen-activated protein kinase (MAPK) signaling pathway, which contributes to disease pathogenesis [1,7,8]. Histopathological assessment should include immunohistochemical staining for CD1a and/or CD207, while molecular testing may identify alterations in the MAPK pathway, including BRAF mutations [7-9]. However, tissue sampling may be nondiagnostic, particularly when the biopsy contains only limited or nonspecific inflammatory changes.

FDG PET/CT may help identify metabolically active lesions suitable for biopsy [7,10]. We report an adult patient in whom a vertebral lytic lesion and diffuse micronodular and nodular pulmonary abnormalities initially suggested granulomatous disease before serial imaging findings raised suspicion for LCH.

Case Presentation

The patient was a 62-year-old woman who initially underwent investigation for chronic lower back pain, which had been present since 2018 and worsened in 2022, leading to the identification of a lytic lesion involving the L4 vertebral body.

A lumbar CT scan performed in December 2021 demonstrated a lytic lesion of the L4 vertebral body without vertebral collapse, prompting an oncological workup (Figure *1*).



FIGURE 1: Lumbar spine CT shows a lytic lesion involving the L4 vertebral body, without significant vertebral body collapse

Right paramedian sagittal CT reconstruction showing a lytic lesion predominantly involving the right side of the L4 vertebral body, with associated cortical disruption and extension into the right pedicle. The white arrow indicates the lesion. No significant vertebral body collapse is observed.

CT, computed tomography

Bone scintigraphy performed in January 2022 demonstrated intense focal uptake corresponding to the L4 lytic lesion, extending into the right pedicle, with a surrounding osteoblastic reaction. No other distant hyperactive lesions were identified. Whole-body FDG PET/CT performed in February 2022 confirmed hypermetabolic uptake in the L4 lytic lesion, as well as multiple bilateral pulmonary micronodules and nodules (Figure *2*).

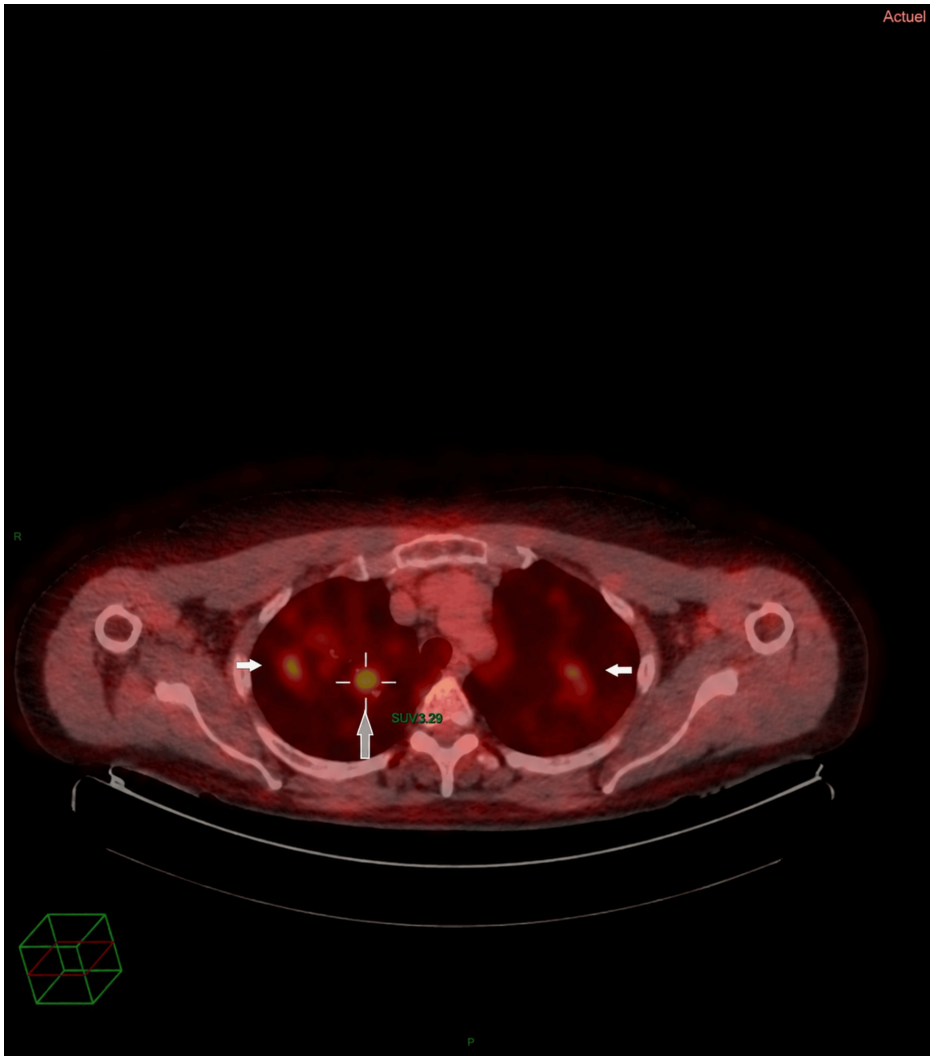


FIGURE 2: Axial fused FDG PET/CT image showing bilateral pulmonary nodular abnormalities with variable FDG uptake

The white-filled arrow indicates metabolically active pulmonary lesions, while the gray-filled arrow indicates one such pulmonary lesion, with a maximum standardized uptake value (SUVmax) of 3.29.

CT, computed tomography; FDG, fluorodeoxyglucose; PET, positron emission tomography

Initial FDG PET/CT demonstrated a hypermetabolic hepatic abnormality near segments VII-VIII. Subsequent contrast-enhanced thoracoabdominal CT did not identify a corresponding suspicious hepatic lesion, although a bilobed hepatic cyst was noted in segment IV. The overall imaging findings raised concern for granulomatous disease, particularly miliary TB or sarcoidosis, while metastatic malignancy was considered as an alternative diagnosis.

At clinical assessment in March 2022, she reported cough and dyspnea. Her body mass index was 27.5 kg/m^2, with no weight loss and a weight gain of approximately 10 kg. She was an active smoker with a 45-pack-year smoking history and had no relevant past medical history. Chest radiography demonstrated diffuse bilateral reticulonodular pulmonary abnormalities, predominantly involving the upper and middle lung fields (Figure *3*).

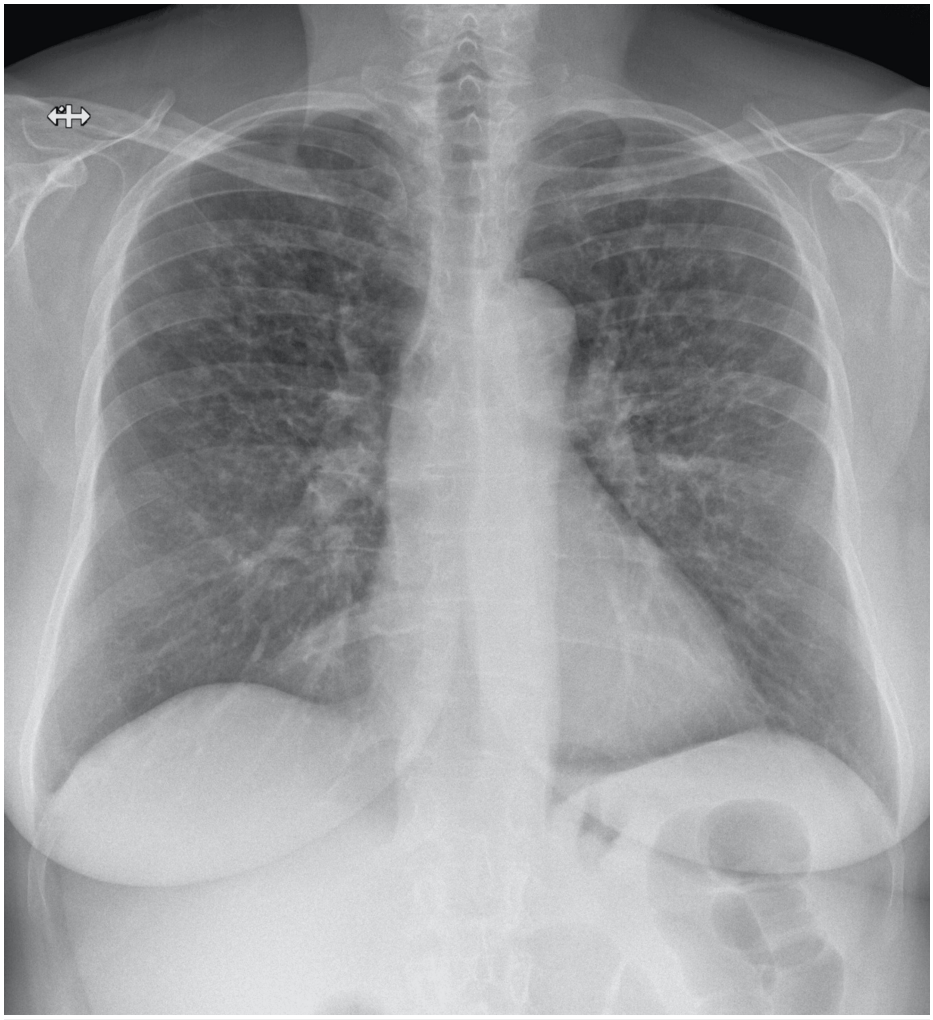


FIGURE 3: Chest radiograph showing bilateral diffuse reticulonodular pulmonary opacities, predominantly involving the upper and middle lung fields

At a subsequent clinical assessment on April 25, 2022, oxygen saturation was 95%, body temperature was 36.0°C, blood pressure was 114/75 mmHg, and heart rate was 85 beats/min. The patient was eupneic at rest, with no adventitious breath sounds on pulmonary auscultation.

Subsequent thoracoabdominal CT confirmed the diffuse pulmonary micronodular distribution, predominantly involving the upper and middle lung fields (Figure *4*), and demonstrated moderate mediastinal lymphadenopathy, without significant interval change in the L4 lytic lesion. No suspicious hepatic lesion corresponding to the previously identified FDG-avid focus was identified on contrast-enhanced CT.

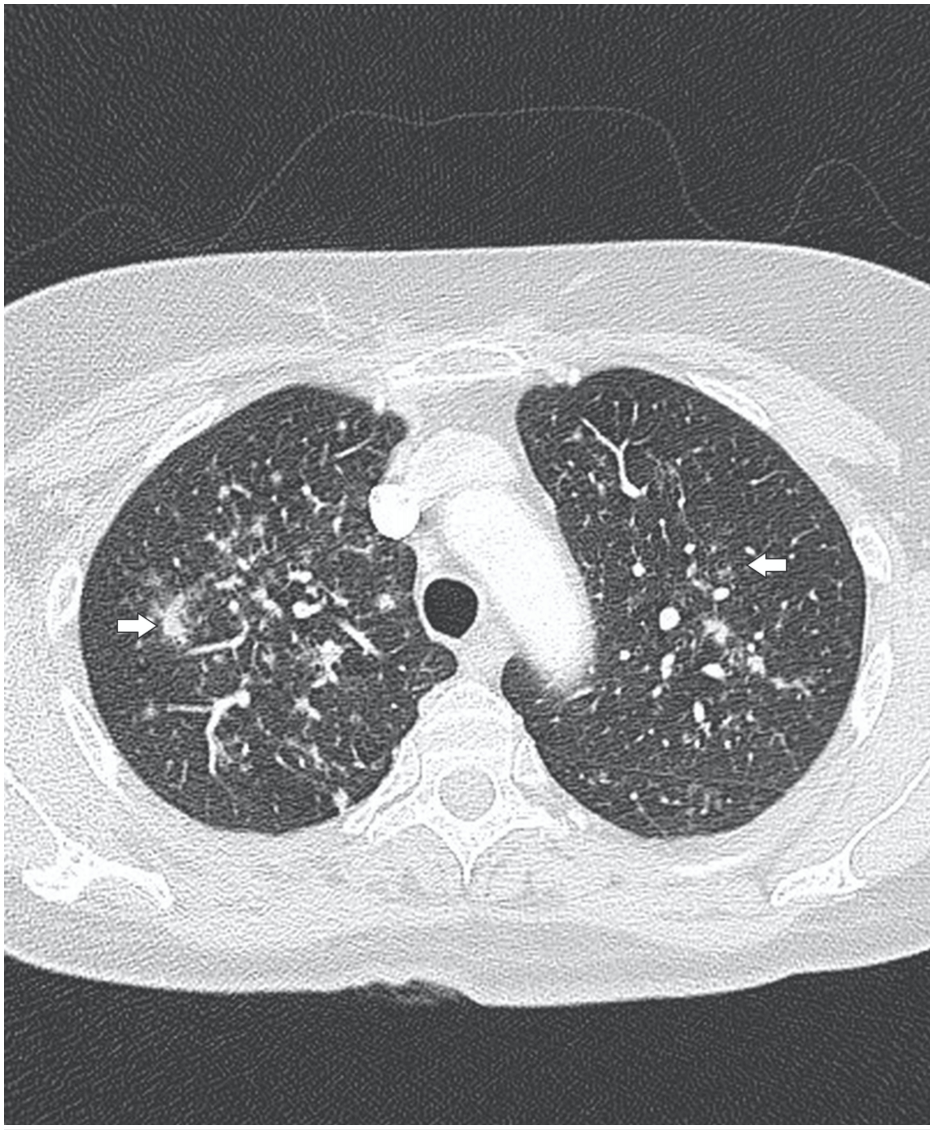


FIGURE 4: Axial chest CT reconstruction in February 2022 showing multiple bilateral pulmonary micronodules and nodules, predominantly involving the upper and mid-lung fields

The diffuse micronodular appearance initially raised suspicion of miliary TB. The straight arrows indicate representative pulmonary nodules and micronodules.

CT, computed tomography; TB, tuberculosis

Spinal magnetic resonance imaging (MRI) revealed no disc destruction, paravertebral abscess, or vertebral collapse.

A right transpedicular biopsy of the L4 lesion performed in March 2022 demonstrated nonspecific intraosseous inflammatory changes, predominantly composed of lymphocytes, with rare eosinophils, numerous macrophages, and occasional multinucleated giant cells. These findings were considered potentially compatible with granulomatous inflammation, although no well-formed granulomas were specifically described. Hemosiderin-laden macrophages were also identified. No necrosis or malignant cells were observed. Periodic acid-Schiff (PAS) and Ziehl-Neelsen staining, as well as immunostaining for *Mycobacterium tuberculosis*, did not demonstrate infectious organisms. CD68 immunostaining confirmed numerous macrophages, while AE1/AE3 did not identify epithelial cells.

Bronchoalveolar lavage and transbronchial biopsy samples were negative on Auramine staining, and subsequent mycobacterial cultures were also negative. Histological examination of the transbronchial lung biopsy initially demonstrated nonspecific chronic interstitial inflammatory changes, with lymphocytes, eosinophils, and numerous intra-alveolar macrophages. No granulomas or malignant cells were identified.

AE1/AE3 did not identify epithelial cells, while CD68 confirmed numerous macrophages.

The microbiological investigations performed on the vertebral biopsy, transbronchial lung biopsy, and bronchoalveolar lavage specimens are summarized in Table *1*. Auramine staining, Xpert MTB/RIF Ultra testing, and prolonged mycobacterial cultures were negative for *M. tuberculosis* in the specimens tested. Additional bacterial, fungal, Legionella, and Pneumocystis investigations of bronchoalveolar lavage were negative. Despite these findings, the QuantiFERON-TB assay was positive.

Specimen	Investigation	Result
L4 vertebral biopsy	Auramine staining	Negative
L4 vertebral biopsy	Xpert MTB/RIF Ultra	Not detected
L4 vertebral biopsy	Mycobacterial culture	Negative after 56 days
Transbronchial lung biopsy	Auramine staining	Negative
Transbronchial lung biopsy	Mycobacterial culture	Negative after 56 days
BAL	Auramine staining	Negative
BAL	Xpert MTB/RIF Ultra	Not detected
BAL	Mycobacterial culture	Negative after 56 days
BAL	Aerobic bacterial culture	Negative
BAL	Legionella culture and *Legionella pneumophila* PCR	Negative
BAL	Direct fungal examination, yeast and fungal cultures	Negative
BAL	Aspergillus antigen	Negative (index 0.07)
BAL	*Pneumocystis jirovecii* testing	Negative
BAL	Influenza, RSV, human metapneumovirus and viral culture	Negative
Blood	QuantiFERON-TB assay	Positive

TABLE 1: Microbiological investigations performed during the initial diagnostic work-up

BAL: bronchoalveolar lavage; MTB: *Mycobacterium tuberculosi*; RIF: rifampicin; PCR: polymerase chain reaction; RSV: respiratory syncytial virus; TB: tuberculosis

Given the miliary-like pulmonary distribution, inflammatory changes observed in the vertebral biopsy, and positive QuantiFERON result, empirical four-drug antituberculous treatment was initiated by the treating infectious disease team in May 2022, despite negative initial microbiological investigations. HIV screening was negative. Clinical follow-up documented appropriate treatment adherence and generally good tolerance, with no significant treatment-related toxicity reported in the available records.

After approximately six weeks of antituberculous treatment, chest radiography showed no significant interval change, although the patient reported stable or slightly improved general well-being. Follow-up FDG PET/CT performed in July 2022 demonstrated a mixed metabolic response. The pulmonary lesions showed low-grade and variable FDG uptake, with a maximum standardized uptake value (SUVmax) of 3.02. The L4 lytic lesion had completely resolved metabolically, whereas a new FDG-avid lytic lesion appeared in the L2 vertebral body, with an SUVmax of 5.69. The previously described hypermetabolic hepatic abnormality in segment VII had also completely resolved. Antituberculous treatment was discontinued on July 22, 2022, after approximately 11 weeks, because of the absence of a favorable overall imaging response and negative mycobacterial cultures from the vertebral and pulmonary specimens.

Subsequent chest CT demonstrated heterogeneous evolution of the pulmonary lesions, with some nodules decreasing in size while others enlarged or newly appeared. Several nodules developed cavitation, and new cystic lesions also developed (Figure *5*). This nodulocystic evolution raised suspicion of pulmonary LCH.

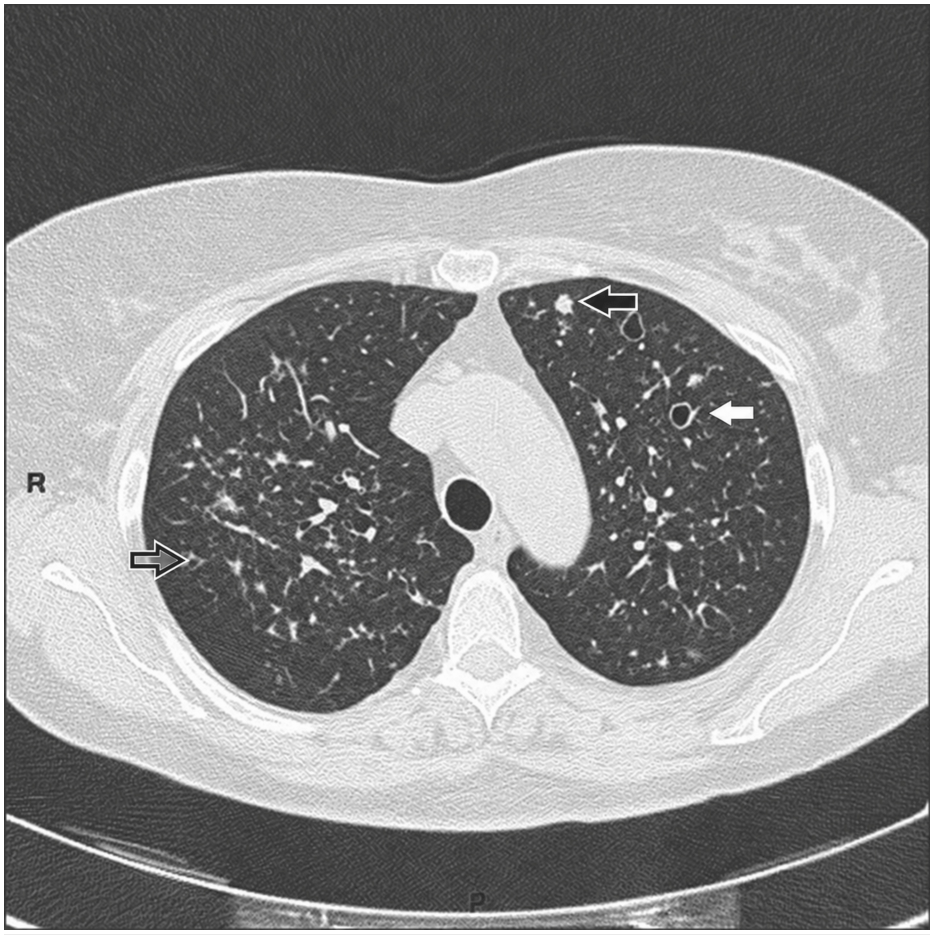


FIGURE 5: Axial chest CT image from July 2022 showing heterogeneous changes in the pulmonary lesions

Some nodules decreased in size, whereas others enlarged or newly appeared, with subsequent development of cavitation and cystic lesions. The white-filled arrow indicates a cyst in the left upper lobe, the black-filled arrow with a white outline indicates a newly appearing nodule in the left upper lobe, and the unfilled arrow with black and white outlines indicates a cavitated nodule in the right upper lobe. The heterogeneous nodulocystic evolution, including cavitation and cyst formation, raised suspicion of pulmonary LCH rather than the initially suspected miliary TB.

CT, computed tomography; LCH, Langerhans cell histiocytosis; TB, tuberculosis

The characteristic nodulocystic evolution of the pulmonary lesions on serial chest CT raised suspicion of pulmonary LCH. Subsequent reassessment of the transbronchial lung biopsy demonstrated numerous CD1a- and S100-positive cells, supporting the diagnosis of pulmonary LCH. CD207 (Langerin) immunohistochemistry was not documented in the available pathology records, and the proportion of CD1a-positive cells was not quantified. The feasibility of additional retrospective CD207 staining could not be established from the available records.

Following smoking cessation, imaging demonstrated marked improvement in the pulmonary abnormalities. Clinical follow-up documented the absence of bone pain.

Molecular analysis of the transbronchial lung biopsy specimen, performed using real-time polymerase chain reaction (Idylla BRAF Mutation Test, Biocartis), identified a BRAF p.V600E/D alteration in January 2023, providing additional molecular support for pulmonary LCH.

Pulmonary function testing performed in June 2024 demonstrated a forced expiratory volume in one second/forced vital capacity (FEV1/FVC) ratio of 79%, an FEV1 of 86% of the predicted value, and a diffusing capacity of the lungs for carbon monoxide (DLCO) of 70% of the predicted value. Hematological investigations revealed mild microcytic anemia, without documented evidence of hematological involvement attributable to LCH. Endocrine investigations included thyroid function testing, with subsequent identification of autoimmune hypothyroidism. Although additional hormonal investigations were performed during follow-up, the available findings did not establish hypothalamic-pituitary

involvement by LCH.

Follow-up chest CT performed in March 2024 demonstrated substantial improvement in the pulmonary abnormalities compared with the 2022 examinations, although residual micronodules persisted predominantly in the upper lung fields.

The main clinical, radiological, diagnostic, and therapeutic events are summarized chronologically in Table 2.

Date	Clinical findings, investigations, and management
2018-2022	Chronic lower back pain since 2018, worsening in 2022 and prompting further investigations
December 2021	Lumbar CT demonstrated a lytic lesion of the L4 vertebral body without vertebral collapse
January 2022	Bone scintigraphy demonstrated intense focal uptake corresponding to the L4 lytic lesion and extending into the right pedicle, with an associated surrounding osteoblastic reaction
February 2022	Whole-body FDG PET/CT demonstrated a hypermetabolic L4 lesion and multiple bilateral pulmonary micronodules and nodules, raising suspicion of granulomatous disease or metastatic malignancy
March 2022	The patient reported cough and dyspnea, without weight loss but with a weight gain of approximately 10 kg. She was an active smoker with a 45-pack-year smoking history. Chest radiography and CT demonstrated bilateral pulmonary micronodules and nodules, predominantly involving the upper and middle lung fields
March-April 2022	Vertebral biopsy demonstrated intraosseous inflammatory changes without identified infectious organisms or malignant cells. Transbronchial lung biopsy initially showed nonspecific chronic inflammatory changes. Initial microbiological investigations were negative, while subsequent mycobacterial cultures also remained negative. QuantiFERON testing was positive
May 2022	Empirical four-drug antituberculous treatment was initiated on May 3, 2022, by the treating clinical team because of suspected miliary TB
July 2022	Follow-up FDG PET/CT demonstrated a mixed metabolic response, with metabolic resolution of the L4 lesion and the appearance of a new FDG-avid L2 lytic lesion. Antituberculous treatment was discontinued after approximately 11 weeks following the absence of a favorable overall imaging response and negative mycobacterial cultures
July-September 2022	Serial chest CT demonstrated heterogeneous evolution of the pulmonary nodules, including regression of some lesions, progression of others, and the development of cavitation and cystic abnormalities, raising suspicion for LCH
September 2022	Pathological reassessment of the transbronchial lung biopsy subsequently identified CD1a- and S100-positive cells, supporting the diagnosis of LCH
December 2022	Following smoking cessation in late 2022, FDG PET/CT demonstrated marked improvement in the pulmonary abnormalities and metabolic normalization of the previously active osseous lesions. Clinical and imaging surveillance was continued without LCH-directed systemic therapy
January 2023	Molecular testing identified a BRAF p.V600E/D alteration, providing additional support for the diagnosis of LCH
March-June 2024	Follow-up chest CT in March 2024 demonstrated substantial improvement in the pulmonary abnormalities compared with 2022, with residual upper-lung-predominant micronodules. Pulmonary function testing in June 2024 showed an FEV_1/FVC ratio of 79%, an FEV_1 of 86% predicted, and a DLCO of 70% predicted

TABLE 2: Timeline of clinical presentation, diagnostic investigations, treatment, and follow-up

CT, computed tomography; FDG, fluorodeoxyglucose; PET, positron emission tomography; LCH, Langerhans cell histiocytosis; FEV1, forced expiratory volume in one second; FVC, forced vital capacity; DLCO, diffusing capacity of the lungs for carbon monoxide; TB, tuberculosis

Discussion

Adult LCH is rare and can present with a wide range of clinical and imaging findings. Pulmonary disease is strongly linked to smoking, but early disease can be difficult to recognize when CT shows only diffuse micronodules or small nodules without cysts [3,4]. In this patient, the initial miliary appearance and the associated lytic vertebral lesion made the diagnosis particularly difficult.

The main differential diagnoses for diffuse micronodular lung disease in this setting include TB and other infections, sarcoidosis, metastatic disease, and smoking-related disorders. The lack of disc destruction, paravertebral abscess, or vertebral collapse on MRI made typical tuberculous spondylitis and an aggressive vertebral metastasis less likely, although these findings were not specific.

The microbiological workup did not support TB. Microbiological investigations of the vertebral and pulmonary specimens were negative for mycobacteria, including Auramine staining, Xpert MTB/RIF Ultra testing, and prolonged mycobacterial cultures. Fungal, bacterial, Legionella, and Pneumocystis testing performed on bronchoalveolar lavage was also negative. However, the QuantiFERON test was positive.

Nevertheless, empirical antituberculous treatment was initiated because of the initial miliary-like CT pattern, intraosseous inflammatory changes potentially compatible with granulomatous disease, and a positive QuantiFERON result.

Although the positive QuantiFERON result contributed to the initial suspicion of TB, interferon-gamma release assays cannot distinguish latent TB infection from active disease. Furthermore, the absence of weight loss and the negative microbiological investigations made the diagnosis uncertain. Nevertheless, empirical antituberculous treatment was initiated by the treating clinical team because of the initial concern for disseminated TB. The subsequent absence of a favorable overall imaging response, together with persistently negative mycobacterial cultures, prompted reconsideration of the initial diagnosis.

The most useful clue came from follow-up HRCT. The pulmonary nodules did not evolve uniformly: some regressed, others appeared or enlarged, and new cavitated nodules and cysts developed. In a smoker, this combination and its upper- and mid-lung predominance are typical of pulmonary LCH [3,4].

The initial biopsy was nondiagnostic. It showed nonspecific intraosseous inflammatory changes with CD68-positive macrophages but did not establish LCH. Subsequent CD1a and S100 immunostaining of the L4 biopsy did not provide additional evidence of LCH [7].

FDG PET/CT helped assess lesion distribution and activity but was not specific. In adult LCH, PET/CT is mainly useful for staging, selecting a biopsy target, and follow-up rather than for diagnosis based on FDG uptake alone [7,10]. The initially observed hypermetabolic hepatic abnormality in segment VII had completely resolved on follow-up FDG PET/CT in July 2022. Although hepatic involvement was considered in the initial assessment of possible multisystem disease, the absence of histological confirmation precluded definitive attribution of this finding to LCH. Additionally, follow-up PET/CT demonstrated metabolic resolution of the L4 lesion and the appearance of a new FDG-avid L2 lytic lesion, indicating changing skeletal metabolic activity.

The vertebral lesions were considered presumptive manifestations of LCH, as the L4 biopsy was nondiagnostic and the newly identified FDG-avid L2 lesion was not biopsied. Alternative diagnoses, including metastatic disease, fracture-related changes, and a paradoxical reaction to antituberculous treatment, could not be definitively excluded. Nevertheless, the negative mycobacterial investigations, characteristic pulmonary evolution, and subsequent pathological and molecular findings favored LCH as a unifying diagnosis. The metabolic normalization of the vertebral lesions following smoking cessation further supported this hypothesis, without establishing causality or confirming skeletal involvement histologically.

Antituberculous treatment was discontinued on July 22, 2022, after approximately 11 weeks, because of the absence of a favorable overall imaging response and negative mycobacterial cultures from the vertebral and pulmonary specimens.

The extensive microbiological workup, summarized in Table *1*, did not provide evidence of active TB or another pulmonary infection. The absence of microbiological confirmation, together with the subsequent imaging evolution, prompted reconsideration of the initial diagnosis. Subsequent identification of a BRAF p.V600E/D alteration provided additional molecular support for LCH [7-9].

Adult LCH should therefore be considered when diffuse pulmonary nodules are associated with lytic bone lesions, particularly in a current or former smoker [6,7].

Approximately 90% of adults with pulmonary LCH are current or former smokers [3,4]. Smoking cessation is a key component of pulmonary LCH management and may lead to stabilization or regression of pulmonary abnormalities [4,7]. Regular clinical assessment, pulmonary function testing, and follow-up imaging are essential to monitor disease evolution. In contrast, patients with progressive pulmonary disease or clinically significant multisystem involvement may require systemic treatment, including chemotherapy or targeted therapies directed against MAPK pathway alterations [7,8]. In the present case, the favorable radiological evolution following smoking cessation supported continued surveillance without systemic therapy.

This case illustrates the importance of reassessing an initial working diagnosis when subsequent imaging

findings are not consistent with the expected disease course. Although the initial pulmonary abnormalities, associated vertebral lesion, and positive QuantiFERON result raised concern for disseminated TB, microbiological confirmation was lacking. Importantly, a positive interferon-gamma release assay does not distinguish latent TB infection from active disease. The heterogeneous evolution of pulmonary nodules, with subsequent cavitation and cyst formation, provided a more characteristic imaging pattern of pulmonary LCH in the context of substantial tobacco exposure. Serial FDG PET/CT additionally demonstrated changing skeletal metabolic activity. These observations, together with targeted pathological reassessment, supported diagnostic reconsideration. The case highlights the complementary contributions of multimodality imaging and histopathology in evaluating atypical presentations of pulmonary LCH. In this patient, no systemic therapy was initiated because of the favorable radiological evolution following smoking cessation, and clinical and imaging surveillance was continued.

Conclusions

Adult LCH should be considered in current or former smokers presenting with upper- and mid-lung-predominant nodules, particularly when serial CT demonstrates cavitation and cyst formation. Associated lytic bone lesions may initially suggest infection or metastatic disease. In this case, the temporal evolution of the pulmonary abnormalities was the key clue leading to diagnostic reconsideration. Careful reassessment of pathology findings and correlation with serial imaging may help avoid diagnostic delays.

Additional Information

Author Contributions

All authors have reviewed the final version to be published and agreed to be accountable for all aspects of the work.

Acquisition, analysis, or interpretation of data: Dulcis I. Burundi

Drafting of the manuscript: Dulcis I. Burundi

Critical review of the manuscript for important intellectual content: Dulcis I. Burundi, Pascale Bohy

Concept and design: Pascale Bohy

Disclosures

Human subjects: Informed consent for treatment and open access publication was obtained or waived by all participants in this study. **Conflicts of interest:** In compliance with the ICMJE uniform disclosure form, all authors declare the following: **Payment/services info:** All authors have declared that no financial support was received from any organization for the submitted work. **Financial relationships:** All authors have declared that they have no financial relationships at present or within the previous three years with any organizations that might have an interest in the submitted work. **Other relationships:** All authors have declared that there are no other relationships or activities that could appear to have influenced the submitted work.

References

1. Khoury JD, Solary E, Abla O, et al.: The 5th edition of the World Health Organization classification of Haematolymphoid tumours: myeloid and histiocytic/dendritic neoplasms. Leukemia. 2022, 36:1703-19. 10.1038/s41375-022-01613-1
2. Liu H, Stiller CA, Crooks CJ, et al.: Incidence, prevalence and survival in patients with Langerhans cell histiocytosis: a national registry study from England, 2013-2019. Br J Haematol. 2022, 199:728-38. 10.1111/bjh.18459
3. Tazi A: Adult pulmonary Langerhans' cell histiocytosis. Eur Respir J. 2006, 27:1272-85. 10.1183/09031936.06.00024004
4. Radzikowska E: Update on pulmonary Langerhans cell histiocytosis . Front Med (Lausanne). 2020, 7:582581. 10.3389/fmed.2020.582581
5. Sharma P, Dhingra KK, Sural S, Mandal AK, Singh T: Langerhans cell histiocytosis masquerading as tuberculosis: a diagnostic dilemma resulting in inappropriate anti-tubercular therapy. Pediatr Blood Cancer. 2009, 53:111-3. 10.1002/pbc.21930
6. Huang WD, Yang XH, Wu ZP, et al.: Langerhans cell histiocytosis of spine: a comparative study of clinical, imaging features, and diagnosis in children, adolescents, and adults. Spine J. 2013, 13:1108-17. 10.1016/j.spinee.2013.03.013
7. Goyal G, Tazi A, Go RS, et al.: International expert consensus recommendations for the diagnosis and treatment of Langerhans cell histiocytosis in adults. Blood. 2022, 139:2601-21. 10.1182/blood.2021014343
8. Emile JF, Cohen-Aubart F, Collin M, et al.: Histiocytosis. Lancet. 2021, 398:157-70. 10.1016/S0140-6736(21)00311-1
9. Lang M, Chang L, Cai H, et al.: BRAF deletion in adult patients with Langerhans cell histiocytosis correlates with multisystem disease and poor outcomes. Clin Cancer Res. 2025, 31:197-204. 10.1158/1078-0432.CCR-24-1802

10. Obert J, Vercellino L, Van Der Gucht A, et al.: (18)F-fluorodeoxyglucose positron emission tomography-computed tomography in the management of adult multisystem Langerhans cell histiocytosis. Eur J Nucl Med Mol Imaging. 2017, 44:598-610. 10.1007/s00259-016-3521-3